Electronic Supplementary Material (ESI) for Journal of Materials Chemistry C.

Understanding photophysical properties of chiral conjugated corrals for organic photovoltaics

Chunyu Liu,[a] Guochun Yang,*[ab] Yanling Si,[c] Youjun Liu,[d] and Xiumei Pan*[a]

a. *Institute of Functional Material Chemistry, National & Local United Engineering Lab for Power Battery, Faculty of Chemistry, Northeast Normal University, Changchun, 130024 Jilin, China.*
b. *Centre for Advanced Optoelectronic Functional Materials Research and Key Laboratory for UV Light-Emitting Materials and Technology of Ministry of Education, Northeast Normal University, Changchun, 130024 Jilin, China.*
**E-mail: yanggc468@nenu.edu.cn*
c. *College of Resource and Environmental Science, Jilin Agricultural University, Changchun, 130118 Jilin, China.*
d. *Aviation University Air Force, 130022 Jilin, China.*

Contents

Index **Page**

Computational details

1. The effect of different DFT functionals on UV-Vis/CD spectra

Here, four DFT functionals including both conventional and range-separated functionals (B3LYP, M05-2X, CAM-B3LYP and LC-BLYP) were selected, which have successfully described the electron transition property.[1, 2] It is found that the computed absorption wavelengths are very sensitive to the used functionals (Figure S1). The main absorption bands of M05-2X, CAM-B3LYP and LC-BLYP functionals are greatly blue-shifted in UV-Vis spectra compared with the experimental ones. The same blue-shifted trend was also observed in simulated CD spectra. Moreover, the line shapes for CD spectra are also different from the experimental ones. These observations might be due to the larger energy gaps (Table S2). However, the results computed with the B3LYP functional are much closer to the experimental results.

2. Finding suitable DFT functionals for first hyperpolarizability calculation

The conventional, long-range, and high HF exchange fractions functionals (B3LYP, CAM-B3LYP, and BH&HLYP) were selected to test the reliability on first hyperpolarizability, which has widely been used in this field.[3] The overestimates β_{tot} value of B3LYP method originates from the incorrect electric field dependence of the "response part" of the exchange-correlation potential, which lacks a linear term counteracting the applied electric field.[4, 5] However, the CAM-B3LYP and BH&HLYP not only moderates the shortcomings of overestimated hyperpolarizabilities but also provides semiquantitative accuracy.[3, 5-8] Moreover, the long-range corrected functionals have become a promising tool for the prediction of NLO properties.[3, 9, 10] Thus, β_{tot} values obtained from the CAM-B3LYP were used.

3. The number of the lowest energy electronic excitations

If the simulated spectra cover the range of experimental measurement, the accuracy of assignment electron transition property and absolute configuration will greatly be enhanced. Here, the 200 lowest energy electron excitations were calculated at the TDB3LYP/6-31G(d,p) level, which is enough to cover experimental spectra. Notably, both length and velocity representations were used to obtain rotational strengths. The velocity-gauge representation of the dipole operator is gauge origin independent.

References

1. B. M. Wong and T. H. Hsieh, *J. Chem. Theory Comput.*, 2010, **6**, 3704-3712.
2. Y. Zhao, N. E. Schultz and D. G. Truhlar, *J. Chem. Phys.*, 2005, **123**, 161103.
3. S. J. A. van Gisbergen, P. R. T. Schipper, O. V. Gritsenko, E. J. Baerends, J. G. Snijders, B. Champagne and B. Kirtman, *Phys. Rev. Lett.*, 1999, **83**, 694-697.
4. W. Y. Wang, N. N. Ma, S. L. Sun and Y. Q. Qiu, *Phys. Chem. Chem. Phys.*, 2014, **16**, 4900-4910.
5. M. Torrent-Sucarrat, J. M. Anglada and J. M. Luis, *J. Chem. Theory Comput.*, 2011, **7**, 3935-3943.
6. P. A. Limacher, K. V. Mikkelsen and H. P. Luthi, *J. Chem. Phys.*, 2009, **130**, 194114.
7. A. Pedone, *J. Chem. Theory Comput.*, 2013, **9**, 4087-4096.
8. D. Jacquemin, E. A. Perpete, M. Medved, G. Scalmani, M. J. Frisch, R. Kobayashi and C. Adamo, *J. Chem. Phys.*, 2007, **126**, 191108.
9. M. de Wergifosse and B. Champagne, *J. Chem. Phys.*, 2011, **134**, 074113.
10. M. J. Peach, A. J. Cohen and D. J. Tozer, *Phys. Chem. Chem. Phys.*, 2006, **8**, 4543-4549.

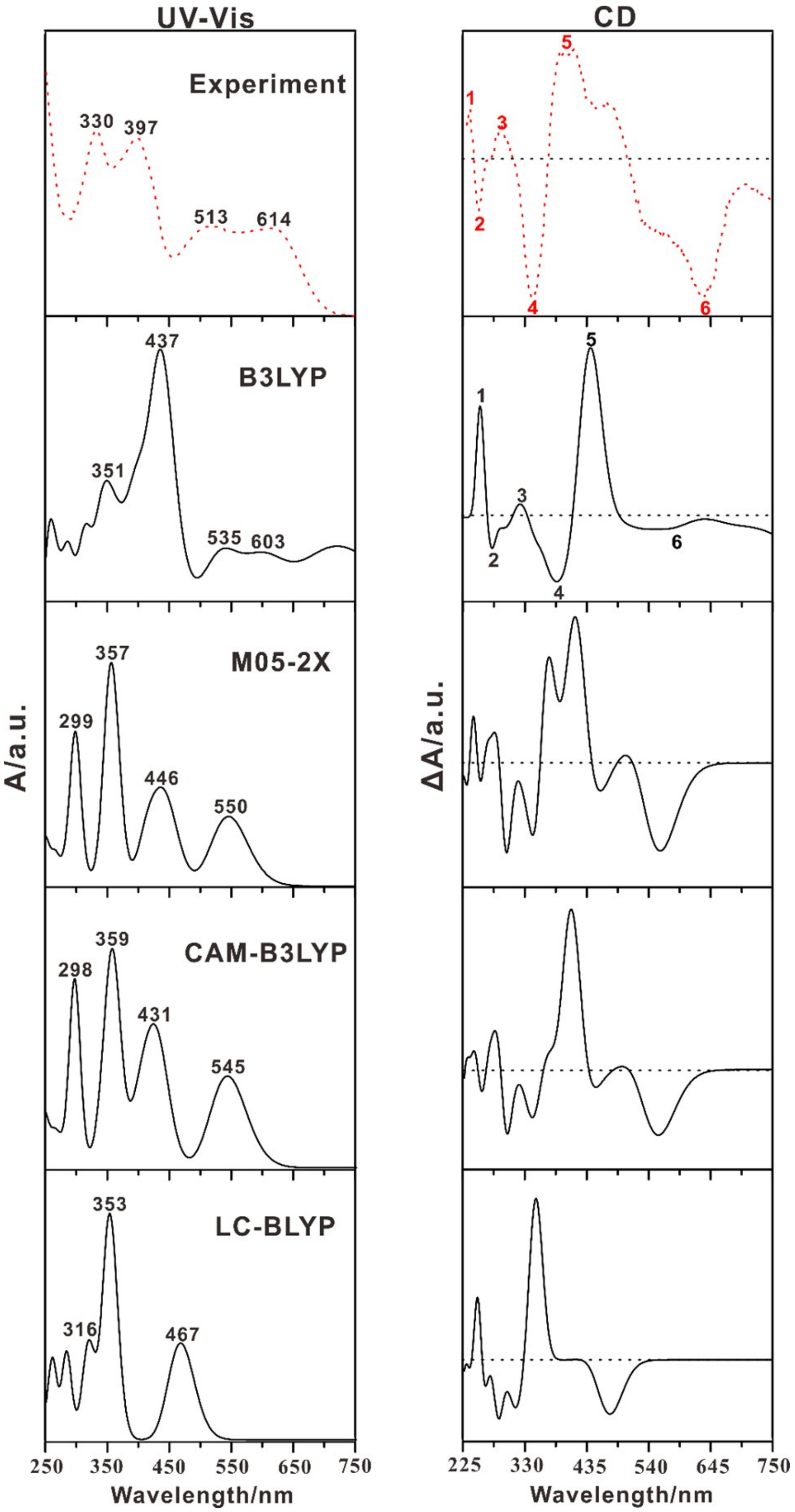

Figure S1. Calculated UV-Vis (left) and CD (right) spectra of compound **1** using four different DFT functionals along with the experimental spectra.

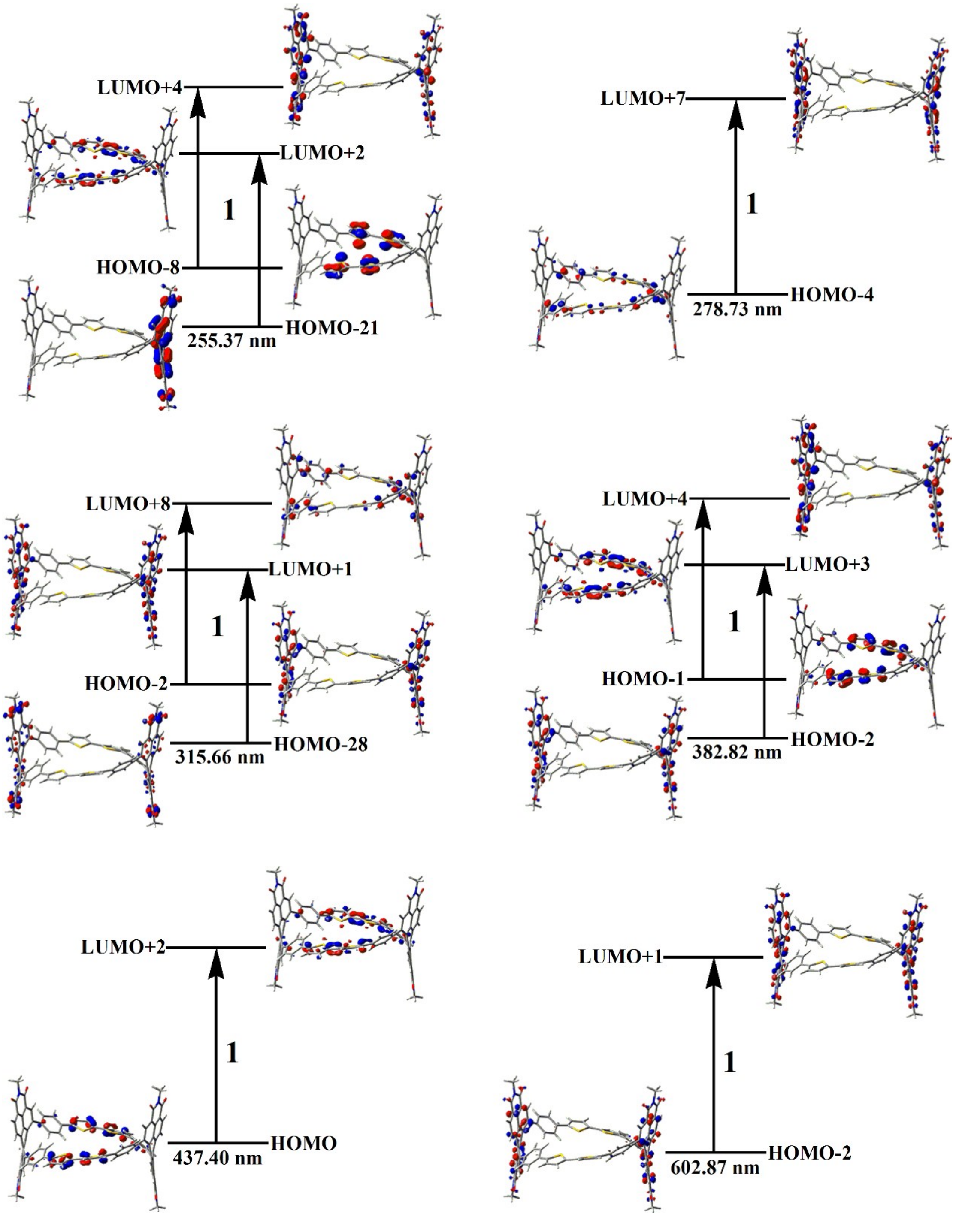

Figure S2. Molecular orbitals involved into the main CD transition of compound **1**.

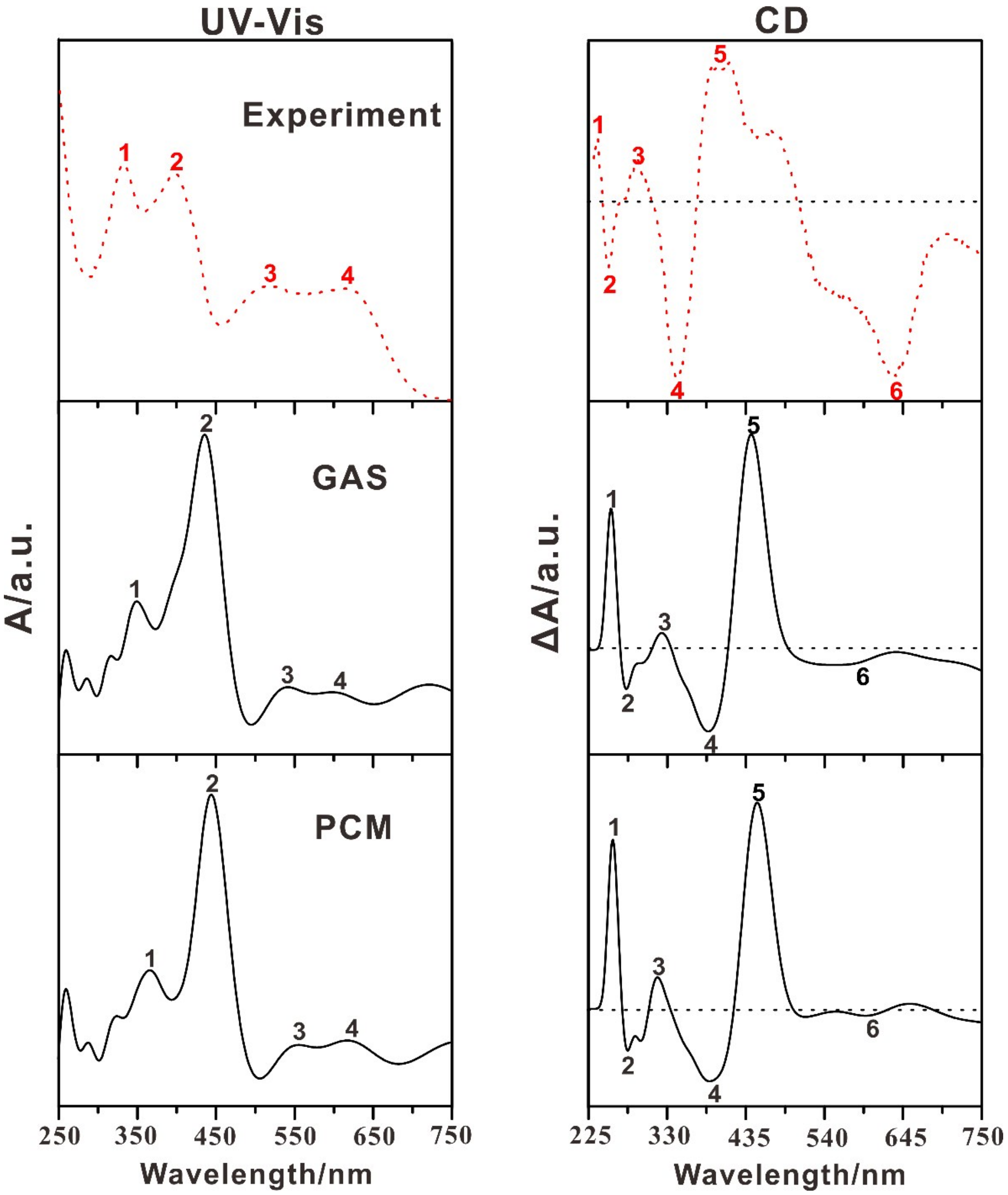

Figure S3. Calculated UV-Vis (left) and CD (right) spectra in both gas and solution phases for compound **1** at the TDB3LYP/6-31G(d,p) level of theory along with experimental spectra.

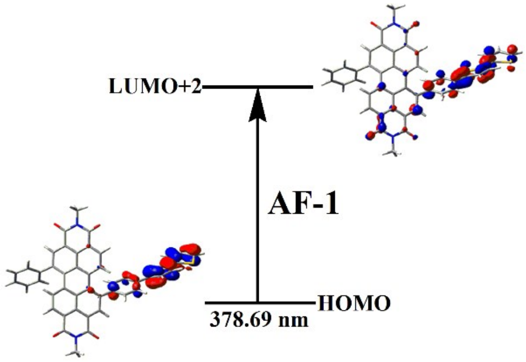
LUMO+2
AF-1
HOMO
378.69 nm

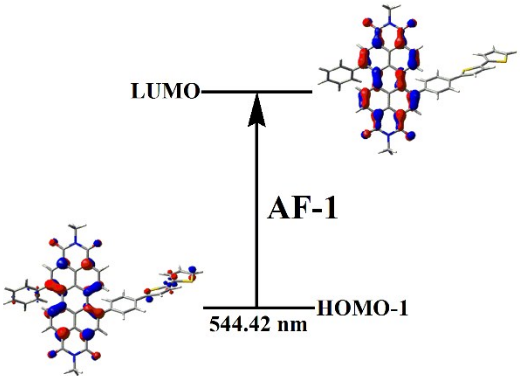
LUMO
AF-1
HOMO-1
544.42 nm

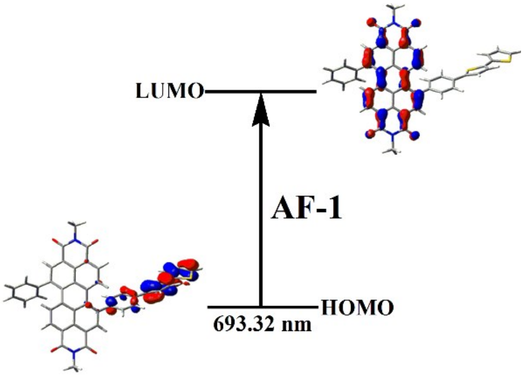
LUMO
AF-1
HOMO
693.32 nm

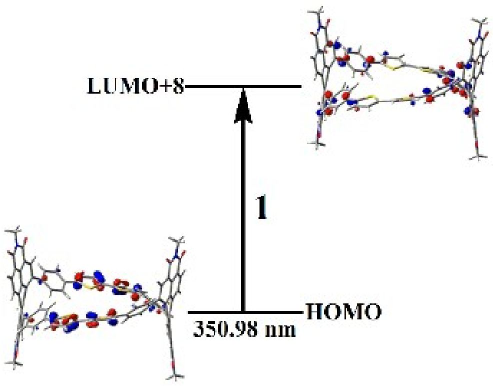
LUMO+8
1
HOMO
350.98 nm

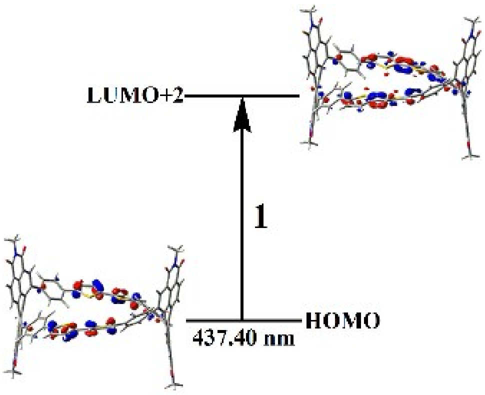
LUMO+2
1
HOMO
437.40 nm

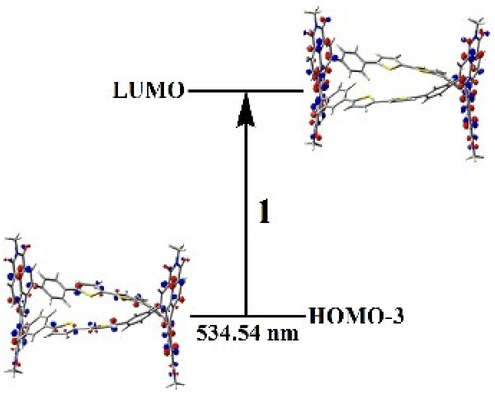
LUMO
1
HOMO-3
534.54 nm

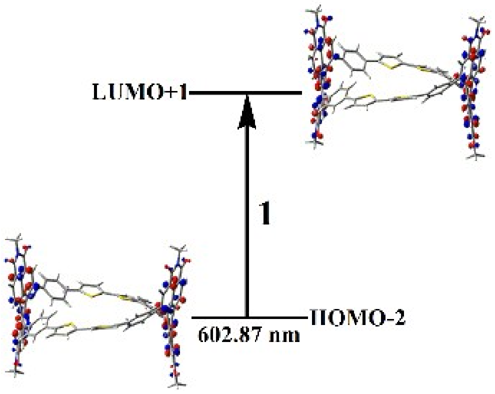
LUMO+1
1
HOMO-2
602.87 nm

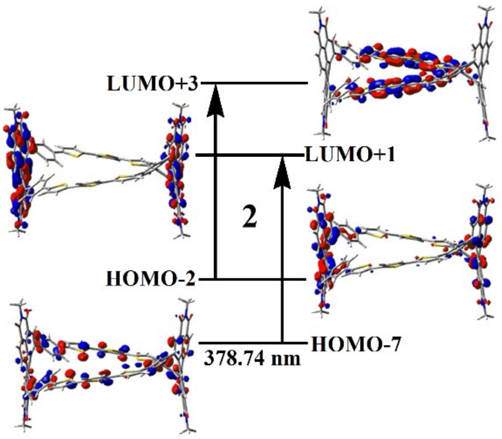
LUMO+3
LUMO+1
2
HOMO-2
378.74 nm
HOMO-7

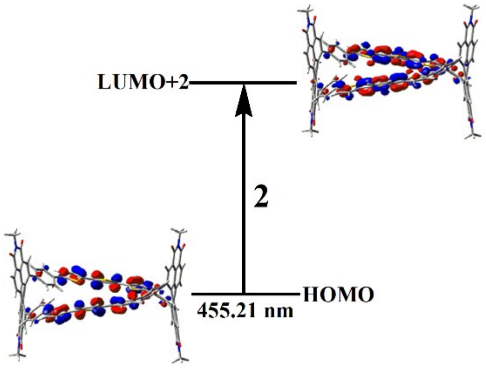
LUMO+2
2
455.21 nm
HOMO

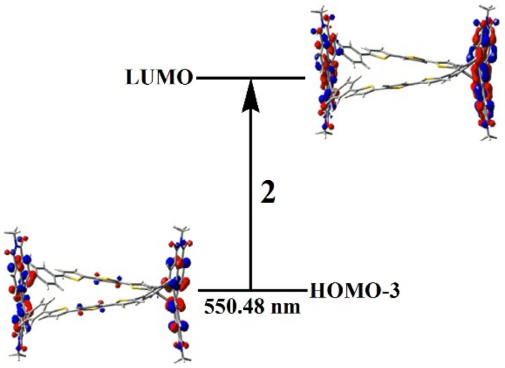
LUMO
2
550.48 nm
HOMO-3

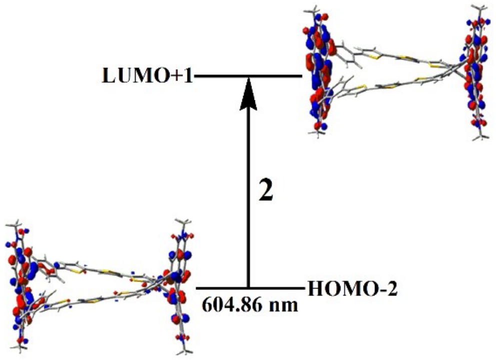
LUMO+1
2
604.86 nm
HOMO-2

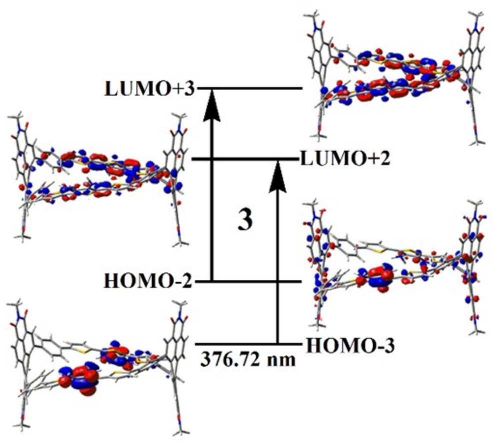
LUMO+3
LUMO+2
3
HOMO-2
376.72 nm
HOMO-3

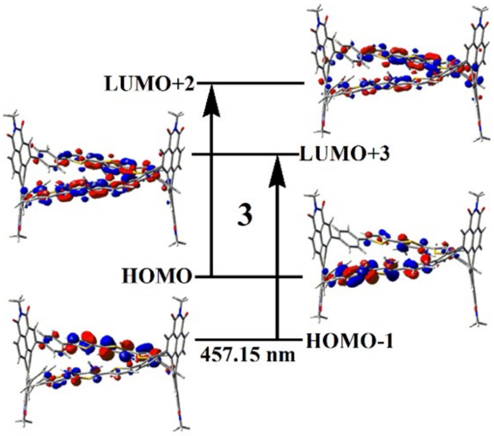
LUMO+2
LUMO+3
3
HOMO
457.15 nm
HOMO-1

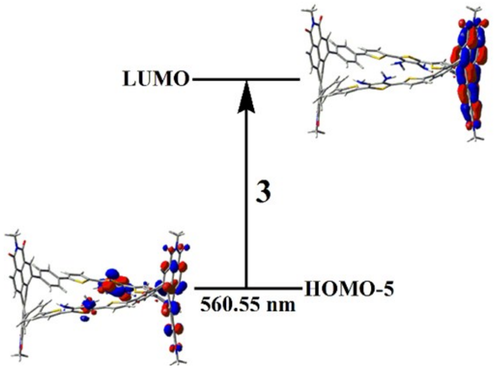
LUMO
3
560.55 nm
HOMO-5

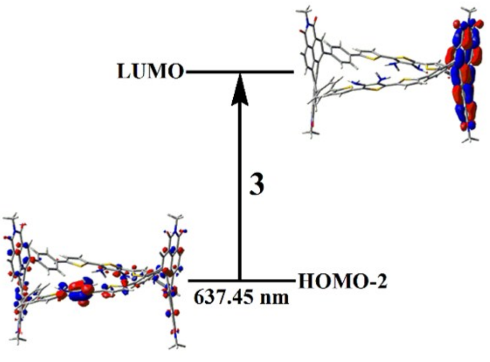
LUMO
3
637.45 nm
HOMO-2

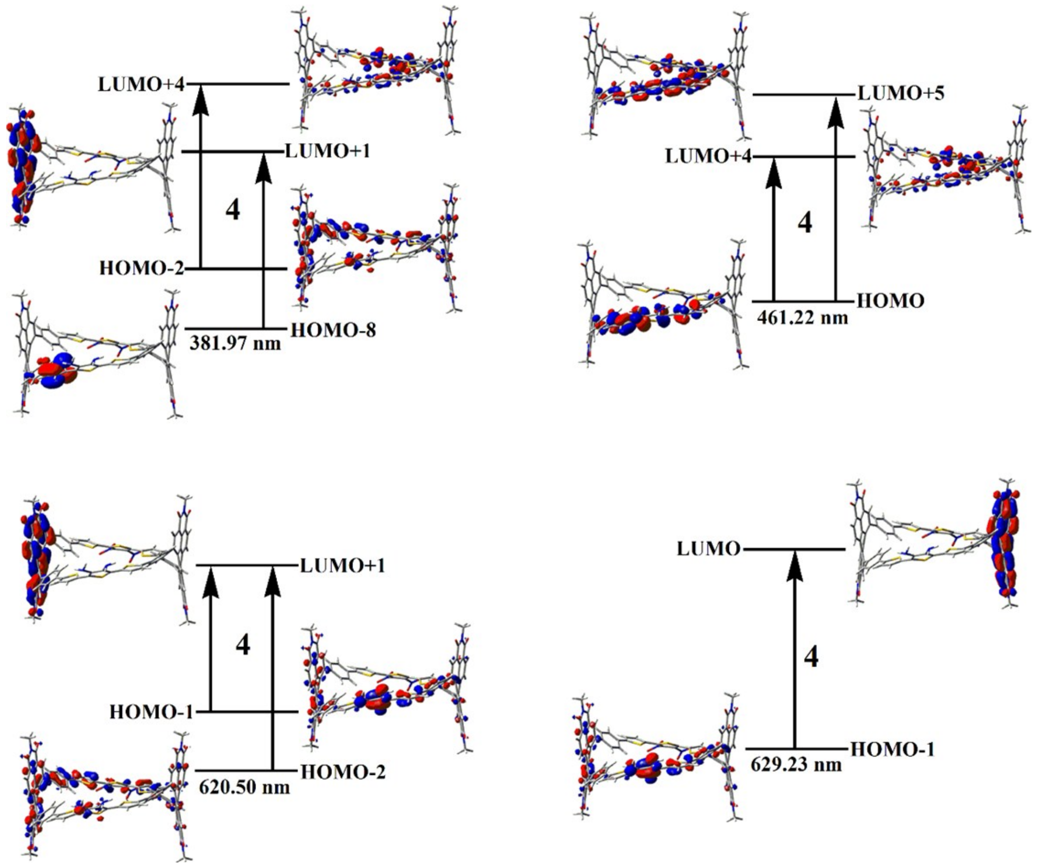

Figure S4. Molecular orbital isosurfaces involved in the main electron transitions of compounds **1-4** and **AF-1** at the TDB3LYP/6-31G(d,p) level of theory.

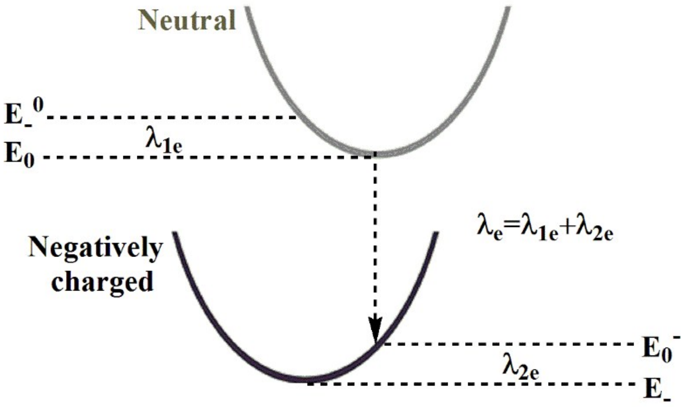

Figure S5. Sketch map of electron reorganization energy.

Table S1. The lowest harmonic frequencies (cm^{-1}) of compounds **1-4** and **AF-1** obtained at B3LYP/6-31G(d,p) level of theory.

Compound	Frequencies
AF-1	10.11
1	6.19
2	5.24
3	5.25
4	4.95

Table S2. Computed HOMO and LUMO energy level and corresponding energy gaps (E_g = LUMO - HOMO) in eV using different functionals at 6-31G(d,p) level for compound **1**.

Functional	HUMO	LUMO	E_g
B3LYP	-5.31	-3.46	1.85
M05-2X	-6.49	-2.91	3.58
CAM-B3LYP	-6.45	-2.56	3.89
LC-BLYP	-7.61	-1.77	5.84

Table S3. The calculated excitation energies, oscillator strengths and rotational strengths for compound **1** in the gas phase at the TDB3LYP/6-31G(d,p) level.

states	eV	λ^a	f^b	Rlength^c	Rvelocity^c
1	1.5537	798.01	0.0625	-1233.5516	-1332.5181
2	1.6487	752.01	0.1277	732.2584	704.6638
3	1.7609	704.10	0.2572	-447.8595	-435.3375
4	1.8063	686.39	0.0000	-0.0060	-0.0059
5	2.0285	611.22	0.0686	884.3278	861.8028
6	2.0566	602.87	0.2315	-913.0286	-947.6130
7	2.3194	534.54	0.3340	-70.8649	-72.5565
8	2.3500	527.58	0.0023	-147.0373	-129.0178
9	2.6318	471.11	0.0000	-0.0302	-0.0300
10	2.6599	466.13	0.0986	-234.9204	-238.7376
11	2.8098	441.26	0.1832	4171.4211	4157.6311
12	2.8346	437.40	1.2545	-1117.7914	-1104.0898
13	2.9256	423.79	0.0730	-406.1867	-384.7900
14	2.9449	421.01	0.0804	468.6256	466.9263
15	3.0478	406.80	0.0085	-6.1332	-5.9138
16	3.0519	406.25	0.0069	-170.4141	-172.7071

17	3.0541	405.96	0.1664	-76.3520	-73.7229
18	3.1165	397.83	0.3419	-404.0185	-402.8515
19	3.1206	397.30	0.0311	-34.8562	-34.4952
20	3.1231	397.00	0.0971	-85.6042	-84.1066
21	3.1297	396.16	0.0000	-1.5018	-0.9536
22	3.1312	395.96	0.0001	-2.2965	-1.7328
23	3.1521	393.34	0.0000	-0.0051	-0.0051
24	3.1575	392.66	0.0693	38.3323	36.6945
25	3.2055	386.79	0.0000	0.0004	0.0002
26	3.2306	383.78	0.0000	-0.2362	-0.2250
27	3.2387	382.82	0.0420	-61.6405	-64.1416
28	3.2686	379.32	0.0002	-22.2676	-20.2866
29	3.2710	379.04	0.0000	-2.8825	-2.2188
30	3.2825	377.71	0.0080	-12.8902	-12.7256
31	3.2883	377.04	0.0453	-157.1464	-152.8139
32	3.2893	376.93	0.0425	-156.0078	-151.8579
33	3.3180	373.67	0.0064	25.3019	22.8487
34	3.3233	373.08	0.0776	-72.2953	-72.4130
35	3.3287	372.47	0.0391	-291.6222	-274.9265
36	3.3367	371.58	0.0000	-0.0161	-0.0153
37	3.3768	367.17	0.0001	-4.2274	-5.5560
38	3.3778	367.05	0.0038	-29.6255	-31.3087
39	3.3945	365.25	0.0000	-0.0679	-0.0631
40	3.4036	364.27	0.0008	-8.2482	-10.6733
41	3.4249	362.01	0.2592	146.7823	144.0608
42	3.4458	359.81	0.0021	15.1784	18.6197
43	3.4472	359.66	0.0205	30.8648	32.0260
44	3.4507	359.30	0.0001	-5.2823	-5.3533
45	3.4538	358.98	0.0000	-0.1732	-0.1517
46	3.4872	355.54	0.0218	-42.1334	-39.4880
47	3.5325	350.98	0.1536	-263.7114	-274.2149
48	3.5334	350.89	0.0002	0.0979	0.0986
49	3.5608	348.19	0.0004	13.3525	13.6914
50	3.5640	347.88	0.0071	-52.0450	-53.6554
51	3.5701	347.28	0.0000	-0.3620	-0.3654
52	3.5706	347.23	0.0661	-45.1085	-43.9356
53	3.5826	346.07	0.0002	-0.4333	-0.4548
54	3.5917	345.20	0.0038	-43.3087	-42.3469
55	3.5954	344.84	0.0550	7.5801	7.8089
56	3.5989	344.51	0.0251	315.1444	307.9324
57	3.6058	343.85	0.1104	-191.9952	-179.5541
58	3.6063	343.80	0.0317	-89.9508	-91.0547
59	3.6175	342.74	0.0288	-18.4120	-18.1763
60	3.6315	341.41	0.0001	-0.5018	-0.5064

61	3.6325	341.32	0.0002	-1.1515	-1.1539
62	3.6411	340.52	0.0001	-0.1304	-0.1185
63	3.6417	340.46	0.0000	-0.1654	-0.1538
64	3.6456	340.09	0.0009	-1.0965	-1.1378
65	3.6484	339.83	0.0437	28.2012	26.7622
66	3.6494	339.74	0.0049	12.5433	12.9524
67	3.6521	339.49	0.0207	17.6518	16.0977
68	3.6633	338.45	0.0000	-0.3106	-0.2496
69	3.6692	337.91	0.0079	27.3704	26.9501
70	3.6827	336.66	0.0000	-0.0316	-0.0322
71	3.7019	334.92	0.0024	-5.2517	-5.0297
72	3.7072	334.44	0.1611	32.7287	30.3910
73	3.7170	333.56	0.0000	0.1783	0.1446
74	3.7191	333.37	0.0035	41.6267	37.2010
75	3.7370	331.78	0.0000	0.7915	0.5139
76	3.7386	331.64	0.0013	45.5153	28.6703
77	3.7695	328.91	0.0065	9.2993	8.3460
78	3.7729	328.62	0.0024	6.0829	5.7813
79	3.7859	327.49	0.0000	-0.2118	-0.2236
80	3.7925	326.92	0.0000	-0.2158	-0.2093
81	3.7966	326.57	0.0010	-31.8510	-41.5590
82	3.8069	325.69	0.0004	-11.0811	-14.5005
83	3.8110	325.33	0.0020	-26.4533	-29.3166
84	3.8189	324.66	0.0005	-8.2575	-9.5778
85	3.8374	323.10	0.0005	-5.4472	-5.8907
86	3.8472	322.27	0.0049	59.1539	49.0443
87	3.8510	321.95	0.0010	-9.6702	-10.5076
88	3.8733	320.10	0.0109	113.1978	112.8512
89	3.8831	319.29	0.0021	28.8976	27.3072
90	3.9172	316.52	0.0000	-0.0077	-0.0082
91	3.9277	315.66	0.0077	268.2117	282.9366
92	3.9310	315.40	0.3840	-138.0318	-136.0962
93	3.9376	314.87	0.0000	-0.1556	-0.1646
94	3.9612	313.00	0.0057	-51.3521	-51.9840
95	3.9747	311.93	0.0085	-99.4215	-103.3685
96	3.9828	311.30	0.0000	-0.2386	-0.2504
97	4.0236	308.14	0.0197	16.5251	16.8386
98	4.0404	306.86	0.0141	-34.8604	-36.3219
99	4.0549	305.77	0.0002	7.2472	4.3460
100	4.0684	304.75	0.0000	-0.0015	-0.0013
101	4.0827	303.68	0.0170	-3.1547	-3.1295
102	4.0989	302.48	0.0005	-10.5138	-13.6326
103	4.1107	301.61	0.0418	-65.6494	-70.2259
104	4.1245	300.60	0.0076	14.3149	15.7417

105	4.1311	300.13	0.0060	102.1823	104.0301
106	4.1344	299.88	0.0000	0.0005	0.0006
107	4.1733	297.09	0.0000	-0.0147	-0.0165
108	4.1819	296.48	0.0077	-18.0673	-22.1166
109	4.1825	296.43	0.0006	0.7943	0.7477
110	4.1854	296.23	0.0004	-2.7373	-2.7689
111	4.1929	295.70	0.0001	0.1597	0.1595
112	4.1933	295.68	0.0000	0.0153	0.0154
113	4.2074	294.68	0.0181	-18.1340	-19.0496
114	4.2229	293.60	0.0198	-52.4893	-48.6629
115	4.2314	293.01	0.0000	-0.0033	-0.0026
116	4.2475	291.90	0.0213	-59.7187	-58.4775
117	4.2560	291.32	0.0032	2.3122	2.1660
118	4.2833	289.46	0.0160	-171.3756	-161.8956
119	4.3050	288.00	0.0031	35.3802	26.8667
120	4.3258	286.61	0.0885	74.9069	77.1609
121	4.3311	286.26	0.1604	201.0251	197.0085
122	4.3583	284.48	0.0000	-0.0019	-0.0019
123	4.3794	283.11	0.0000	-0.0808	-0.0793
124	4.3920	282.29	0.0259	-40.7384	-39.8724
125	4.4024	281.63	0.0000	-0.0333	-0.0318
126	4.4059	281.40	0.0016	7.7883	6.6615
127	4.4175	280.67	0.0108	-27.0241	-22.3659
128	4.4260	280.13	0.0172	1.8283	1.6820
129	4.4456	278.89	0.0000	-0.2056	-0.2711
130	4.4482	278.73	0.0064	-96.0342	-103.2113
131	4.4602	277.98	0.0096	-83.4743	-99.6712
132	4.4622	277.85	0.0005	-4.0923	-4.8527
133	4.4720	277.25	0.0111	-42.6630	-37.8301
134	4.4928	275.96	0.0041	6.7357	6.6068
135	4.4969	275.71	0.0046	-40.0050	-19.1588
136	4.5094	274.95	0.0081	7.4123	6.8985
137	4.5279	273.82	0.0017	-7.4093	-7.7639
138	4.5397	273.11	0.0024	-8.8865	-8.6798
139	4.5533	272.29	0.0113	-47.8996	-51.2445
140	4.5570	272.07	0.0001	0.1824	0.0138
141	4.5640	271.66	0.0001	-1.5141	-1.5632
142	4.5825	270.56	0.0001	3.0492	2.5184
143	4.5852	270.40	0.0000	3.0201	2.3336
144	4.5901	270.11	0.0009	-1.9314	-1.8331
145	4.5928	269.95	0.0007	-1.4604	-1.3729
146	4.5963	269.75	0.0030	1.3840	1.2092
147	4.6024	269.39	0.0862	-149.8385	-144.4337
148	4.6177	268.50	0.0395	-6.5791	-6.5654

149	4.6206	268.33	0.0215	-59.2701	-56.6843
150	4.6314	267.71	0.0024	47.0495	46.5839
151	4.6482	266.74	0.0359	37.6317	35.7566
152	4.6491	266.68	0.0093	3.5039	3.7219
153	4.6504	266.61	0.0074	-11.9586	-10.7197
154	4.6576	266.20	0.0015	-17.7834	-22.5517
155	4.6610	266.00	0.0000	-0.0034	-0.0033
156	4.6661	265.71	0.0086	1.6159	1.1640
157	4.6703	265.48	0.0085	20.3951	18.1837
158	4.6715	265.41	0.0029	10.4440	9.9409
159	4.6734	265.30	0.0000	0.0669	0.0648
160	4.6845	264.67	0.0017	18.9052	18.3406
161	4.6915	264.27	0.0014	58.1334	67.6528
162	4.6994	263.83	0.0029	-10.8647	-9.8640
163	4.7019	263.69	0.0017	-9.4214	-8.5152
164	4.7101	263.23	0.0002	-0.2716	-0.3252
165	4.7123	263.11	0.0001	-0.2526	-0.3034
166	4.7151	262.95	0.0000	-0.0002	0.0003
167	4.7256	262.37	0.0117	58.4163	61.8660
168	4.7290	262.18	0.0010	-11.7435	-11.2601
169	4.7409	261.52	0.0128	15.7839	15.3023
170	4.7497	261.04	0.0038	45.5777	35.8139
171	4.7549	260.75	0.0011	-2.3313	-2.2731
172	4.7563	260.68	0.0145	-29.7848	-28.8788
173	4.7638	260.26	0.0000	-0.0480	-0.0466
174	4.7866	259.02	0.1379	-376.2629	-362.1839
175	4.7878	258.96	0.0000	-0.0062	-0.0125
176	4.7912	258.77	0.0005	5.8479	1.5817
177	4.8025	258.17	0.0126	93.4796	77.7471
178	4.8111	257.70	0.0863	201.6974	197.3589
179	4.8171	257.38	0.0000	0.0064	0.0097
180	4.8224	257.10	0.0012	21.3838	25.3418
181	4.8261	256.90	0.0157	137.6336	135.2793
182	4.8303	256.68	0.0415	387.3769	384.3523
183	4.8322	256.58	0.0001	-0.5612	-0.5609
184	4.8328	256.55	0.0023	-8.7875	-8.7779
185	4.8361	256.37	0.0029	48.1460	44.9424
186	4.8411	256.11	0.0000	0.0319	0.0440
187	4.8550	255.37	0.0488	162.1297	161.4106
188	4.8595	255.14	0.0277	106.9210	105.3347
189	4.8667	254.76	0.0004	0.5786	0.6000
190	4.8695	254.62	0.0190	39.4622	39.9830
191	4.8696	254.61	0.0007	0.1241	0.1323
192	4.8714	254.51	0.0067	15.3778	15.5248

193	4.8738	254.39	0.0040	-3.8103	-3.2149
194	4.8756	254.30	0.0003	-2.1544	-1.3063
195	4.8765	254.25	0.0001	0.2514	0.2455
196	4.8769	254.23	0.0010	-0.8688	-0.7088
197	4.8828	253.92	0.0073	82.7121	80.7383
198	4.8904	253.52	0.0060	11.1776	11.1766
199	4.8984	253.11	0.0088	58.7883	52.6110
200	4.9024	252.90	0.0167	95.5203	90.1189

[a] λ in nm. [b] Oscillator Strengths. [c] R values (in 10^{-40} esu^{2}cm^2) using the velocity-gauge representation and length-gauge representation of the electric dipole operator.

Table S4. Calculated excitation energies (ΔE_{ge}, eV), absorption wavelengths (λ, nm) along with experimental data (in parentheses), oscillator strengths (*f*), and major contributions of the other main absorption bands for the compounds **1-4** and **AF-1**.

Compound	ΔE_{ge}	λ	f	Major contribution
AF-1	2.28	544.42	0.387	H-1→L (98%)
1	2.32	534.54(513)	0.334	H-3→L (98%)
	3.53	350.98(330)	0.154	H→L+8 (66%)
2	2.25	550.48	0.301	H-3→L (98%)
	3.27	378.74	0.463	H-7→L+1 (43%) H-2→L+3 (28%)
3	2.21	560.55	0.222	H-5→L (92%)
	3.29	376.72	0.426	H-2→L+3 (23%) H-3→L+2 (15%)
4	2.00	620.50	0.239	H-1→L+1 (46%) H-2→L+1 (20%)
	3.25	381.97	0.223	H-2→L+4 (32%) H-8→L+1 (15%)

Table S5. Calculated bond-length alternation (BLA, in Å) (going from the neutral to the anion state) of compounds **1-4** and **AF-1**.

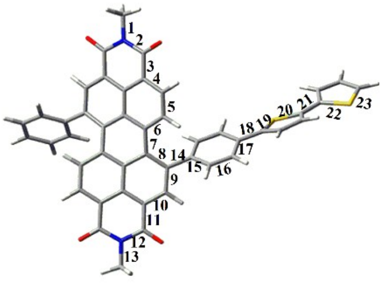

AF−1

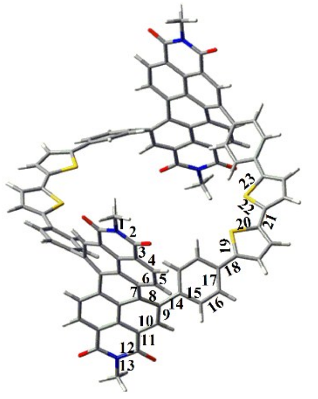

1

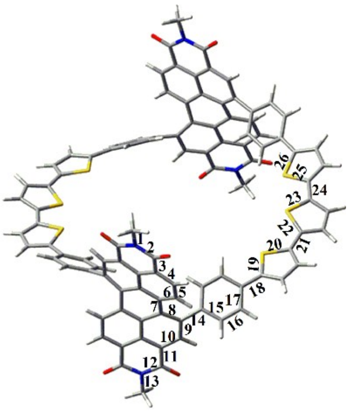

2

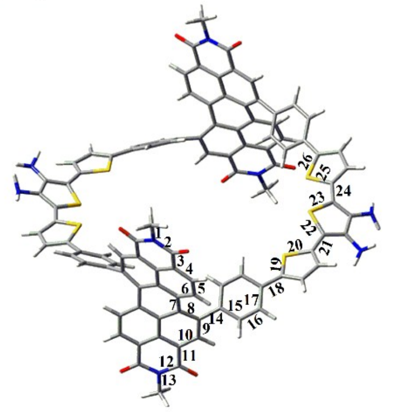

3

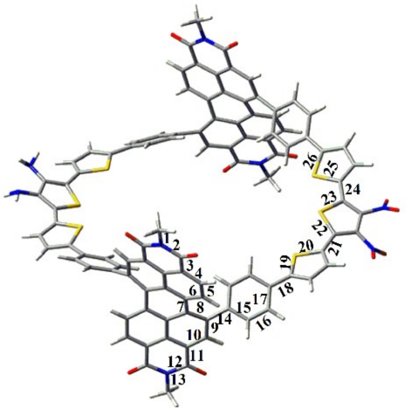

4

Bonds	BLA(**AF-1**)	BLA(**1**)	BLA(**2**)	BLA(**3**)	BLA(**4**)
1	-0.006	-0.003	-0.003	-0.003	-0.003
2	0.006	0.003	0.002	0.002	0.003
3	**-0.019**	**-0.010**	**-0.010**	**-0.010**	**-0.009**
4	**0.016**	**0.008**	**0.008**	**0.008**	**0.008**
5	**-0.017**	**-0.008**	**-0.008**	**-0.009**	**-0.008**
6	**0.019**	**0.009**	**0.009**	**0.010**	**0.009**
7	**-0.022**	**-0.011**	**-0.011**	**-0.012**	**-0.011**
8	**0.023**	**0.011**	**0.011**	**0.011**	**0.011**
9	**-0.016**	**-0.009**	**-0.008**	**-0.009**	**-0.008**
10	**0.014**	**0.007**	**0.007**	**0.007**	**0.007**
11	**-0.019**	**-0.010**	**-0.009**	**-0.010**	**-0.010**
12	0.005	0.003	0.002	0.002	0.003
13	-0.006	-0.003	-0.003	-0.003	-0.003
14	-0.004	-0.001	-0.001	-0.001	-0.002
15	0.002	0.000	0.001	0.000	0.002
16	-0.001	0.000	0.000	-0.001	-0.001
17	0.000	0.000	-0.001	0.000	0.000
18	0.000	-0.001	0.000	0.001	-0.002

19	0.001	0.001	0.000	0.001	0.001
20	0.003	0.001	0.000	0.001	0.002
21	-0.001	-0.001	0.000	0.001	-0.002
22	0.003	0.001	0.001	0.000	0.002
23	0.002	0.001	0.001	0.001	0.002
24			-0.001	0.001	-0.003
25			0.001	0.000	0.003
26			0.001	0.000	0.001